Backward and forward electron emission measurements for MeV H^0 projectiles incident on thin carbon foils: correlation with the charge state of the emergent projectile

Z. Vidović, A. Billebaud*, M. Fallavier, R. Kirsch, J.-C. Poizat and J. Remillieux

Institut de Physique Nucléaire de Lyon, IN2P3-CNRS / Université Claude Bernard Lyon-1
F-69622 Villeurbanne Cedex, France

PACS numbers: 79.20 Rf, 34.50 Dy.

ABSTRACT

We have performed projectile-by-projectile measurements of backward and forward secondary electron emission of thin carbon foils under impact of MeV H^0 projectiles. The emitted electrons were detected in coincidence with the protons or the neutrals emerging from the target. We have used a very thin target for which we know that, at energies above 2 MeV, the emergent neutrals are essentially transmitted, i.e. they have kept their electron throughout the target. In these conditions the emission yields measured in coincidence with emergent neutrals are found lower than for protons of the same velocity but the reduction factor is not the same for backward and for forward emission. We show that this can be explained by the screening of the proton charge by the electron during the H^0 - target interaction. We have observed other effects related to forward electron emission: if the H^0 projectile emerging from the foils results from an electron capture event taking place close to the exit surface, the forward emission is enhanced (at energies above 500 keV) by the contribution of Auger electrons resulting from the rearrangement of the carbon atoms ionized in the capture events. For H^0 projectiles ionized in the target we have used the statistics of the number of forward emitted electrons to deduce the probability for an incident electron to be transmitted through a very thin target and to produce cascade electrons.

*Present address: Institut des Sciences Nucléaires, 38026 Grenoble Cedex, France

I. INTRODUCTION

Kinetic electron emission of solids under impact of MeV ions has been studied for a long time both experimentally and theoretically. The phenomenon is usually described as a three-step process involving the production of excited electrons, the transport of the liberated electrons in the solid, including cascade multiplication, and the transmission through the surface. To this surface phenomenon it is convenient to associate the length λ_{SE}, called the secondary electron mean escape depth, first introduced by Sternglass [1]. Whereas the secondary electron emission from solids is rather well understood for incident protons, the situation is still far from being elucidated for other projectiles as heavy ions or molecular and cluster ions. This is mainly due to the dynamic evolution of the projectiles when penetrating into the solid, as the modification of the ion charge state or the breakup into fragments of incident polyatomic ions. Then experimental data specific of a particular state of the projectile can shed light on the resulting electron emission process for composite projectiles that dissociate into multiple components inside the mean electron escape depth. To this end we have undertaken a series of experiments on the statistics of the electron emission induced by various hydrogen projectiles passing through thin solid targets.

In a recent paper [2] we had reported on ion-by-ion measurements of backward electron emission from a thin carbon foil bombarded by various MeV hydrogen projectiles. The goal was to compare the yields and statistics of the kinetic electron emission induced by H^+, H^0, H^- and H_2^+ projectiles of the same velocity. The main conclusions were the following: i) the backward emission yield and statistics are the same for incident H^- and H_2^+ projectiles above 500 keV / u, which strongly suggests that the backward emission mainly originates from distant collisions of the projectiles with target electrons. ii) the backward electron emission for impact of H^0 projectiles is not the simple addition of the respective contributions of the

incident electron and proton. We had performed a calculation based on the successive contributions of a neutral hydrogen atom (from the surface to the depth λ_0, the mean free path length for H^0 ionization) and of two independent particles, one proton and one electron (from λ_0 to infinite depth). The comparison of the experimental and calculated energy dependences of the electron yield allowed us to estimate the value of λ_{SE}, the secondary electron mean escape depth. The calculation was in particular based on the estimation of the electron emission induced by a "frozen" H^0 atom. For this we had assumed that the secondary electron yield is proportional to the H^0 energy loss rate which was calculated using a formulation proposed by Kaneko [3] for frozen H-like ions.

In the present study our main goal is to determine experimentally the electron emission yield from thin carbon foils traversed by frozen MeV H^0 atoms. It can be expected that electron emission due to frozen H^0 projectiles be specific, both at incidence and emergence. From an experimental point of view, the necessary (but not sufficient) condition for the traversal of a thin foil by a frozen H^0 projectile is that the projectile be detected after emergence as a neutral. However an emergent H^0 atom may also result from electron capture by a proton near the target exit surface, which is expected to give also particular electron yields. With very thin targets, fast enough neutral projectiles can travel throughout the target in a frozen charge state. With thicker targets (or at lower energies) the emergent beam reflects charge equilibrium and the emergent neutrals are due to electron capture.

We have measured backward and forward electron emission induced by H^+ and H^0 incident projectiles of energies ranging from 0.27 to 2.2 MeV. The secondary electron detection was triggered by the detection of either a proton or an H^0 atom emerging from the carbon foil. We describe the experimental set-up in Section II and present the experimental results in Section III. In Section IV we discuss the dependence of the electron emission yields upon the origin of the emergent H^0 projectiles. Besides the backward and forward electron yields resulting from the interactions of frozen H^0 atoms, particular effects in the forward emission related to projectile charge changing processes are explained by additional contributions of

the Auger deexcitation of target atoms or by the role of electrons lost by the incident neutral projectiles.

II. EXPERIMENTAL

The experimental set-up used to perform projectile-by-projectile measurements of the number of electrons emitted by the entrance and emergence surfaces of a thin foil traversed by fast projectiles is shown in **Fig. 1**.

The H^+ beam was delivered by the 2.5 MV Van de Graaff accelerator of our Institute. Neutral hydrogen beams were obtained from electron capture collisions undergone by protons of the primary beam in the residual gas of the upstream part of the beam line, the proton beam being bent off by means of a removable magnet. The intensity of the H^+ or H^0 beams was adjusted to a low value (about one thousand projectiles per second) by means of two collimators located before the target chamber. Two carbon foils, that we will call the thin and the thick target, were mounted on a target holder. Their thicknesses had been determined by energy loss measurements with He beams and found to be 145 ± 15 Å for the thin one and 1180 ± 120 Å for the thick one (the evaporated carbon density is taken to be 1.65 g / cm^3 [4]).

The electron detection system consists of two grounded silicon detectors D_B and D_F facing the two sides of the 45°-tilted carbon target maintained at a negative potential - V_0 ($V_0 \approx 20$ kV). The secondary electron collection by these two detectors is performed in coincidence with the detection of the transmitted projectile in one of two other silicon detectors D_1 and D_2, that are used according to the needed angular acceptance of the detection. This coincidence method meets three essential requirements: i) the secondary electron spectra are freed from spurious background counts due to spontaneous electron emission. ii) the detection of an emergent particle without detection of an electron is used to get W_0, the probability that no electron be emitted. iii) the electron detection can be restricted

to secondary electrons associated with the passage of a projectile emerging with a particular property. Moreover the transverse electric field produced by a pair of parallel plates located in front of the target allows us to control the impact location of the charged particle beams when the target is biased. In our energy range the emergent beam is mainly a proton beam (the neutral fraction is for instance 5 10^{-4} at 1 MeV). When the coincidence is triggered by the transmitted beam, for example viewed by D_1, we are allowed (due to the small neutral fraction) to consider that this is equivalent to a coincidence measurement with transmitted protons. On the other hand, coincidence measurements with emergent H^0 projectiles are performed by using a second pair of parallel plates, located behind the target, to bent off the transmitted protons. In this case the emergent H^0 projectiles are detected by D_2. In addition, as the target bias leads to an energy difference eV_0 between emergent protons and neutrals that is larger than the D_2 energy resolution, the trigger signal from the projectile detector was restricted to the proper energy window.

The energy spectra delivered by each of the two electron detectors are made of peaks corresponding to electron multiplicities. However, as electrons (of energy eV_0) can be backscattered out from the detector, laying there only a fraction of their energy, the detector response to the simultaneous arrival of n electrons is not a Gaussian peak centered at energy neV_0, but presents a tail on the low energy side. From a simulation of an electron energy spectrum based on the response of the detector to the arrival of a single electron of energy eV_0, one can deduce the electron number distribution, and its mean value which is the electron yield. An example of electron energy spectrum was given in Ref. 2 and the fitting procedure is described in details separately [5]. The overall accuracy of the values of the experimental yields is better than 5 %. When the electron energy spectrum can be obtained only with a low counting statistics, it is no more possible to apply safely the fitting procedure: this happens for example when electrons are detected in coincidence with a transmitted H^0 atom. In this case, in order to determine the electron yield, we used the energy - multiplicity scale conversion obtained from an

energy spectrum with a high counting statistics in the same experimental conditions (for example in coincidence with protons instead of neutrals).

In the next sections the various experimental electron yields will be named as follows: B and F indices stand for backward and forward emission, respectively; and the incident and the selected emergent projectiles are given in parentheses. For example $\gamma_B(H^0,H^+)$ is the backward yield for a target bombarded with H^0 atoms when measured in coincidence with emergent H^+ ions.

III. RESULTS

A. Backward electron emission

In **Fig. 2** the measured backward secondary electron yields induced by H^+ ions and H^0 atoms passing through 145 Å and 1180 Å thick carbon foils are shown as a function of the incident energy.

For incident protons for which the measurements were performed in coincidence with transmitted protons, no dependence of the backward yield on the target thickness is observed. This shows, as expected, that λ_{SE}, the mean electron escape depth, is smaller than the thin target thickness 145 Å, in agreement with our previous estimate (~ 100 Å) [2]. For protons the proportionality between the electron yield and the energy loss rate is well established. For a given material the proportionality coefficient between the yield and the material stopping power S_e is usually called the material parameter Λ_B. In Fig. 2 the energy dependence of $\gamma_B(H^+,H^+)$ is shown to be fitted by a curve giving the product Λ_B $Se(H^+)$ for a Λ_B value of 0.44 ± 0.02 Å / eV (with standard $S_e(H^+)$ values [6]), which is in agreement with the values usually obtained in previous experiments.

For H^0 incident projectiles, we show the backward electron yields $\gamma_B(H^0,H^+)$ and $\gamma_B(H^0,H^0)$ measured in coincidence with emergent protons and emergent H^0 atoms, respectively. The $\gamma_B(H^0,H^+)$ yields are found to be independent of the target

thickness, a result which is due to the fact that the H^0 mean free path λ_0 in solid carbon, that varies from about 8 Å at 0.27 MeV up to 34 Å at 2.2 MeV (see Section IV), is much shorter than λ_{SE} and then, than the thickness of the thin target. As previously discussed [2], the observed enhancement of the yields with respect to the proton curve results from the contribution to the secondary electron production of the projectile electron freed in the H^0 ionization process, the contribution of the H^0 atoms being limited because of the small value of λ_0 compared to λ_{SE}.

When secondary electrons are counted in coincidence with emerging H^0 atoms, the energy dependence of the backward yield induced by H^0 projectiles notably differs from the previous one. First, below about 1.25 MeV, the $\gamma_B(H^0,H^0)$ yields are the same for the two targets and are also equal to the $\gamma_B(H^0,H^+)$ yields. But for increasing energies above 1.25 MeV, the $\gamma_B(H^0,H^0)$ yield of the thin target drops quickly and reaches values lower than the $\gamma_B(H^+,H^+)$ yield, down to a factor two for the maximum energy. These findings are related to the two possible origins for emergence of H^0 projectiles from the target: H^0 atoms may be produced by successive projectile electron loss and target electron capture processes in the target, but may also be transmitted after traversal through the target in a frozen charge state. If the incident beam reaches charge equilibrium in the target, the emergent H^0 atoms result from electron capture events occurring near the exit surface, i.e. much beyond the mean escape depth for backward emission, and the backward yield does not depend on the charge state at emergence. This is what is observed with the $\gamma_B(H^0,H^0)$ yields for the thin target at incident energies below 1.25 MeV. It would have been also observed at higher energies with the thick target, but the measurements would have been very difficult (and also useless) due to the very small H^0 fraction at equilibrium above 1.5 MeV. On the other hand, if the emergent H^0 atoms have been transmitted through the target without ionization, the backward electron yield (and the energy loss rate) are expected to be lower than for H^+ ions because of the screening of the projectile nuclear charge

by the bound electron. The discussion in Section IV will show that it is the case for our measurements performed with the thin carbon foil at high energies.

B. Forward electron emission

The energy dependences of the forward yields, measured simultaneously with the backward yields of Fig. 2, are shown in **Fig. 3**. Like for the backward yield, $\gamma_F(H^+,H^+)$ is found to be the same for the two targets. The curve of Fig.3 expressing the proportionality of the electron yield to the carbon stopping power for protons ($\gamma_F(H^+,H^+) = \Lambda_F\ S_e(H^+)$) corresponds to a Λ_F value of 0.49 ± 0.02 Å / eV. For the thick target the forward yields measured with emergent protons do not depend on the incident projectile charge state ($\gamma_F(H^0,H^+) = \gamma_F(H^+,H^+)$), which was expected. For the thin carbon foil and for energies higher than 1.0 MeV, the forward yield $\gamma_F(H^0,H^+)$ does not follow any more the stopping power curve. The observed yield enhancement is due to the fact that projectile electrons lost in H^0 ionization have enough energy to have a high probability of being transmitted through the target and of inducing cascade electrons that may leave the target.

As for the forward yields $\gamma_F(H^0,H^0)$ measured in coincidence with emergent H^0 atoms, the energy dependence reflects the effects of the variation of the relative fractions of reconstituted and transmitted H^0 atoms in the total emergent H^0 flux. Above 1.25 MeV, as for backward yields, the forward yields obtained with the thin target decrease with energy faster than in the proton case. For 2.2 MeV the measured yield is below the proton curve by a factor 0.85 (to be compared later with the factor 0.5 obtained for backward emission). For energies ranging between 0.5 and 1.25 MeV, where all the emerging H^0 atoms result from target electron capture near the exit surface, an enhancement of the forward yield is observed for both target thicknesses. The additional contribution to secondary electron production results from the electron capture process, that, on the average, takes place at a distance to the exit surface equal to λ_0, the H^0 mean free path. In this

velocity range, H^+ projectiles capture mainly carbon K - shell electrons and the resulting vacancies are filled essentially through emission of Auger electrons.

All these particular effects in H^0 atom interactions in solids observed on the backward and forward electron yields of thin carbon targets are discussed in more details in the following Section.

IV. DATA ANALYSIS AND DISCUSSION

A. Transmission of H^0 atoms through a thin target

As mentioned in Section III, in the case of a very thin target, the electron yields measured in coincidence with neutral outgoing projectiles must be explained by the presence of two kinds of H^0 atoms in the total flux of H^0 atoms leaving the target. When a foil of thickness d is bombarded by a H^0 beam of energy E, the neutral fraction in the emergent beam can be written [4]:

$$\Phi_0(E,d) = \frac{\sigma_c}{\sigma_l + \sigma_c} + \frac{\sigma_l}{\sigma_l + \sigma_c}\exp\left(-(\sigma_l + \sigma_c)Nd\right) \qquad (1)$$

where N is the atomic density of the target (Nd = 1.7 10^{17} at/cm^2 for the thin carbon foil tilted to 45°), and σ_l and σ_c are the electron capture and loss cross sections, respectively. If one considers that in our velocity range σ_l is much larger than σ_c, $\Phi_0(E,d)$ can be simply written:

$$\Phi_0(E,d) = \frac{\sigma_c}{\sigma_l} + \exp(-\sigma_l Nd) \qquad (2)$$

The first term represents the equilibrium value and corresponds to H^0 atoms that have suffered at least one cycle of successive electron loss and electron capture and that will be called "reconstituted" H^0 atoms and noted H^0_r. The second term corresponds to H^0 atoms transmitted through the target in a frozen charge state, that we note H^0_t. In the energy range of our experiments, the energy dependences of the loss and capture cross sections can be deduced from experiments performed with solid carbon targets and gaseous compounds [4,7]. As the two cross section

sets do not differ greatly, we used the analytical formula, derived from a compilation of experimental data and given by Nakai et al [8], to calculate the energy dependence of the two H^0 fractions for the thin target, that are shown in **Fig. 4**. Below 1 MeV, the neutral fraction at emergence corresponds to charge equilibrium, and is then composed essentially of reconstituted H^0 atoms. Above 1 MeV the fraction of transmitted neutrals is no more negligible and becomes a significant part of the emergent H^0 beam, that increases with energy from 5 % at 1 MeV up to 95 % at 2 MeV. Note that the Φ_{0r} values shown in Fig. 4 are equal to the neutral fraction at emergence from the thick target at all energies.

B. Electron emission induced by frozen H^0 projectiles

Our high energy data show clearly that the electron emission induced by frozen H^0 projectiles is reduced with respect to the electron emission induced by incident or emergent protons of the same velocity. Basically the effect results from the mutual screening of the projectile electron and proton, which reduces the effective charge. It is of course tightly connected to the rate of electronic energy loss of the projectile.

The Bethe stopping power formula for bare ions has been extended to the case of partially stripped ions by Kim and Cheng [9] and an analytical formula has been proposed by Kaneko [3] for hydrogenlike ions in a frozen charge state, when the projectile is assumed to stay in its ground state. Recent measurements of the stopping power of thin carbon foils for 10.4 MeV H^0 have confirmed the calculated values [10]. The carbon stopping power for 2 MeV frozen H^0 projectiles is calculated to be 0.56 times smaller than for protons. From this value and from the backward and forward yields measured at 2.0 and 2.2 MeV, one deduces averaged values for the proportionality parameters Λ^0_B and Λ^0_F: $\Lambda^0_B = 0.41 \pm 0.06$ Å/eV and $\Lambda^0_F = 0.71 \pm 0.02$ Å/eV. These values have to be compared with the Λ values deduced from proton measurements: $\Lambda_B = 0.44 \pm 0.02$ Å/eV and $\Lambda_F = 0.49 \pm 0.02$ Å/eV. As the comparison between Λ values for protons and for neutrals reveals

different behaviors for backward and forward emissions, we will describe each case separately.

First we consider backward emission: Since the Λ^0_B and Λ_B values are nearly equal, this common value can be considered as a parameter independent of the hydrogen projectile charge state, that correlates backward electron emission to stopping power. The energy dependence of the backward yield $\gamma_B(H^0,H^0_t)$ corresponding to transmitted H^0 atoms has been calculated using the Λ_B value for protons (0.44 Å/eV) and is shown as a curve in **Fig. 5**. In order to reproduce the experimental energy dependence $\gamma_B(H^0,H^0)$ we need also to know the backward yields $\gamma_B(H^0,H^0_r)$ due to reconstituted emergent H^0 atoms. As it is clear that the backward yield does not depend on the charge state at emergence, then $\gamma_B(H^0,H^0_r)$ is equal to $\gamma_B(H^0,H^+)$. Using the fractions of reconstituted and transmitted H^0 projectiles shown in Fig. 4, the energy dependence of the backward electron yield $\gamma_B(H^0,H^0)$ for H^0 atoms entering and leaving the target can be written as follows:

$$\gamma_B\left(H^0,H^0\right)=\gamma_B\left(H^0,H^+\right)\left(\frac{\sigma_c}{\sigma_l}\right)+\gamma_B\left(H^0,H_t^0\right)\exp(-\sigma_l Nd) \qquad (3)$$

The results of the calculation, shown in Fig. 5, are in good agreement with the measured energy dependence.

As for the forward electron yields, the above calculation shows that the Λ^0_F value, although smaller than the proton value, is much larger than it could be expected from the reduction of the stopping power. The explanation must be searched by considering in more details the interaction of H^0 projectiles with target electrons. In this respect it is convenient to compare electron emission induced by protons and transmitted H^0 projectiles in terms of the ratios γ_F / γ_B. In the general case, the difference between backward and forward electron yields of thin targets is due to the role of primary δ-electrons: resulting from close projectile-electron collisions, they transfer their large initial kinetic energy to many electrons in a cascade multiplication process. The δ-electrons are initially ejected in a forward direction, which leads then to γ_F / γ_B. ratios above unity. Nevertheless the effect is limited because the relative contribution of δ-electrons is small. For protons the

experimental value of the ratio $\gamma_F(H^+,H^+)$ / $\gamma_B(H^+,H^+)$ is about 1.1 in the whole energy range.

For frozen H^0 atoms the experimental value of the ratio $\gamma_F(H^0,H^0_t)$ / $\gamma_B(H^0,H^0_t)$ is 1.6. Among the collisions between a H^0 projectile and the target electrons, the distant collisions with impact parameters larger than a few times a_0 (the Bohr radius) are essentially suppressed by mutual screening of projectile electron and proton. The close collisions of the projectile electron with target electrons are also suppressed since they would not be compatible with the survival of the projectile bound state. Finally the role of the projectile electron in the electron emission process is only to screen the proton. As a consequence, electron emission induced by frozen H^0 projectiles results mainly from small impact parameter collisions of the projectile proton with target electrons. Then, the relative contribution of resulting δ-electrons, that are forward emitted (see above), is much larger than in the proton case, which leads to a higher ratio γ_F / γ_B. This explains why the "H^0 frozen charge state" effect on electron emission is smaller for forward than for backward emission.

C. Forward electron emission by reconstituted H^0 atoms

Forward electron emission induced by reconstituted H^0 atoms can be cleanly observed either with incident protons or with incident neutrals when the emergent beam is charge equilibrated. In the course of our experiments, devoted to incident H^0 projectiles, it is clear from Fig. 4 that the above condition is fulfilled for the thin target below 1.0 MeV and for the thick target on the whole energy range.

In order to explain the electron emission enhancement observed between 0.5 MeV and 1.5 MeV we must consider the dominant mechanisms for electron capture by a proton in the energy range of our experiments: Auger processes involving valence band electrons of the solid and shell processes where the proton captures an electron from a deep level of a target atom [11]. The capture of a valence electron prevails at low energy with a cross section falling off

monotonously with increasing energy. Capture of an electron from a given inner shell presents a maximum cross section for a proton velocity equal to the corresponding orbital velocity. Theoretical cross sections for shell processes can be calculated using the velocity scaling law deduced from an Oppenheimer-Brinkman-Kramers approach [12]. For K - electron capture, the calculated velocity dependence reproduces quite well the experiments. For carbon atoms (K - shell binding energy: U_K = 284 eV), K - electron capture is the dominant process for proton energies above ~ 300 keV. The deexcitation of the resulting ionized carbon atoms takes place essentially through Auger decay (C fluorescence yield $\omega_K = 2\ 10^{-3}$).

As the emergence of a reconstituted H^0 atom from the target must result from a capture event taking place at the mean distance λ_0 from the exit surface ($\lambda_0 \approx 20$ Å at 1 MeV), the deexcitation of the ionized carbon atom by Auger effect contributes also to the forward electron emission through the Auger electron itself or through the electron cascade it can initiate. Detection of Auger electrons in coincidence with charge-changing projectiles had been already used to measure inner shell capture cross sections in ion - atom collisions with gaseous targets [13]. In our case, where the mean escape depth λ_{SE} is larger than the H^0 mean free path λ_0, the electron yield $\gamma_F(H^0,H^0_r)$ is the sum of various contributions due to the changing nature of the projectile over λ_{SE}: secondary electrons are produced by H^+ ions over a mean depth (λ_{SE} - λ_0) and by H^0 atoms in frozen charge state over the mean depth λ_0, The carbon Auger electrons produced over the same depth λ_0 can excite secondary electrons and eventually escape the solid. The yields $\gamma_F(H^0,H^0)$ (equal to $\gamma_F(H^0,H^0_r)$) and $\gamma_F(H^0,H^+)$, measured at 1.0 and 1.25 MeV for the thick target and at 1.0 MeV for the thin target, differ by a value close to unity (see Fig. 3). As the isotropically produced Auger electron itself contributes at most for 0.5, our result shows that the contribution of cascade electrons is significant, in spite of the fact that Auger electrons are produced close to the exit surface.

As a final remark, the 270 keV data point is found below the proton curve. This can be explained if one considers that at this energy the dominant capture process involves valence electrons, which does not produce energetic electrons. Then, the

only effect of the capture is the screening of the proton along the mean path λ_0 before emergence, that lowers the forward yield with respect to the proton value.

D. Forward emission by projectile electrons

While for the thick target bombarded by H^0 atoms the forward electron yields measured in coincidence with emerging protons follow the energy dependence curve of the yields induced by incident protons ($\gamma_F(H^0,H^+) = \gamma_F(H^+,H^+)$), a deviation from this curve, in the case of the thin target and for energies higher than 1.0 MeV, shows up clearly in Fig.3. The enhanced forward electron yield results from the secondary electrons produced by projectile electrons freed in the H^0 ionization process with a velocity nearly equal to the proton velocity. In a study by Kroneberger et al [14] of the secondary electron emission from thin carbon foils bombarded by 1.2 MeV H^0 projectiles, the contribution of the electrons lost by the projectiles to the forward yield had been already observed for target thicknesses smaller than 5 $\mu g / cm^{-2}$. Using the yields measured at 1.25 MeV with the thin target (due to the 45° tilt angle, the projectile path length corresponds to 3.4 $\mu g / cm^{-2}$), we obtain a ratio $\gamma_F(H^0,H^+) / \gamma_F(H^+,H^+)$ of 1.25, that agrees with the interpolation of the data shown in Fig.5 of Ref. [14].

Owing to the large electron loss cross section, the H^0 projectiles lose their electron very rapidly: for example 80% of 2 MeV incident H^0 projectiles have lost their electron at a depth of 50 Å in carbon. The lost electrons may suffer large angular deflections in successive scattering events on target atoms, but their probability for passing through the target is not negligible for H^0 energies between 1 and 2.2 MeV, for which the electron ranges get larger than the target thickness [15, 16]. When a projectile electron leaves the target, the total number of detected electrons includes the electrons produced by the emergent proton, the electrons produced by the emergent projectile electron and the projectile electron itself. In this case it is reasonable to assume that the projectile electron and the proton

interact as independent projectiles near the exit surface. In spite of the rule stating that identical particles cannot be distinguished from each other, it is convenient to consider that the projectile electron is always included in its outgoing electron production. In these conditions the forward electron yield of the thin target for H^0 projectiles at a given energy can be written:

$$\gamma_F(H^0,H^+) = \gamma_F(H^+,H^+) + T_e\, \gamma_F(e_{proj}). \qquad (4)$$

In this relation $\gamma_F(H^+,H^+)$ is the forward yield for protons of the same velocity, T_e is the probability for incident projectile electrons to be transmitted through the target and $\gamma_F(e_{proj})$ is the mean number of forward emitted electrons per transmitted projectile electron. The yield $\gamma_F(e_{proj})$ includes the projectile electron and the mean number $\gamma_F^{SE}(e_{proj})$ of cascade electrons it has produced ($\gamma_F(e_{proj}) = 1 + \gamma_F^{SE}(e_{proj})$). The measured statistical distributions of forward emitted electrons allow us to determine the values of T_e and $\gamma_F(e_{proj})$ in the following way: as we consider that the emergent projectile electron and proton are independent, the measured forward electron distribution $W_n(H^0,H^+)$ is the convolution product of the measured distribution $W_n(H^+,H^+)$ by the distribution of the number of electrons due to the projectile electron. This distribution, that we call $W'_n(e_{proj})$, can be calculated. The details of the calculation giving $W'_n(e_{proj})$ can be found in Ref. 2 where a similar calculation had been performed.

As an example, **Fig. 6** shows the $W_n(H^0,H^+)$ and $W_n(H^+,H^+)$ electron distributions measured with 2.2 MeV projectiles passing through the thin target, and the distribution $W'_n(e_{proj})$ that is deduced from the two previous ones. In this distribution the term $W'_0(e_{proj})$ is equal to the probability of "zero" forward electron emission due to the interaction of the projectile electron with the target. From the above statement it follows that $W'_0(e_{proj}) = 1 - T_e$. The distribution $W'_n(e_{proj})$, after removal of the first term $W'_0(e_{proj})$ and normalisation to unity, is called $W_n(e_{proj})$, the distribution of the number of electrons due to the transmitted projectile electrons.

The mean value of the distribution $W_n(e_{proj})$, which is found here to be 2.4, is equal to $\gamma_F(e_{proj})$. The corresponding mean number of cascade electrons $\gamma_F^{SE}(e_{proj})$

is then equal to 1.4. When applied to experimental data obtained between 1.25 and 2.2 MeV, the same process leads to values of $\gamma_F(e_{proj})$ approximately constant, as shown in **Fig. 7**. The fact that $\gamma_F(e_{proj})$ does not depend on the incident energy (in our energy range) can be explained by the large energetic and angular spreads of the lost projectile electrons when they approach the exit surface. On the contrary, the deduced values of T_e, also given in Fig. 7, increase with the incident energy, which is not surprising. The concept of range in matter for electrons of energies below 1 keV is questionable. Nevertheless, one can estimate from Ref.15 that the value of 200 Å, equivalent to the thickness of the 45°-tilted target, corresponds to the range of electrons of 600 eV (1.1 MeV / u). This is in agreement with our observation that projectile electrons transmitted through the target are detected for incident energies above 1.0 MeV.

The result of this study is that the difference between the $\gamma_F(H^0,H^+)$ and $\gamma_F(H^+,H^+)$ yields from a thin target increases with energy, as shown in Fig. 3, and that it is mainly due to the increase of the transmission probability T_e, the number of cascade electrons being independent of energy. Moreover it is worth noting that from our experiment with H^0 projectiles we can deduce the distribution of the number of forward emitted secondary electrons due to an incident electron, which would be very difficult to obtain in an experiment performed directly with an incident electron beam.

V. CONCLUSION

The main results of this experimental study deal with the electron emission from a thin carbon target traversed by undestructed MeV H^0 projectiles: electron emission yields are smaller than for protons of the same velocity, the reduction being caused by the screening of the proton charge by the projectile electron, as for energy loss. Observed differences between backward and forward emission point out the part of energy loss that is suppressed by screening effects. Moreover we

have measured forward emission for emergent H^0 atoms resulting from electron capture in the target: at low energy the yield is found lower than for emergent protons, that is again due to screening, and larger for higher energies when the Auger rearrangement of carbon K - shell vacancies produces extra electrons. At last we have used the observed emission statistics to determine the transmission probability of incident electrons lost by H^0 projectiles.

This study shows how ion-by-ion measurements of the statistics of secondary electron emission can be a powerful tool in the study of ion-solid interaction processes, specially when performed in coincidence with transmitted projectiles that have interacted in the target in a particular way. Such studies could be usefully extended, for example to polyatomic projectiles or to particles channeled in a thin crystal.

References

[1] E.J. Sternglass, Phys. Rev. **108**, 1 (1957).

[2] A. Billebaud, M. Fallavier, R. Kirsch, J.C. Poizat, J. Remillieux and Z. Vidovic, Phys. Rev. A **55**, 1124 (1997).

[3] T. Kaneko, Phys. Rev. A **43**, 4780 (1991).

[4] M.J. Gaillard, J.C. Poizat, A. Ratkowski, J. Remillieux and M. Auzas, Phys. Rev. A **16**, 2323 (1977).

[5] Z. Vidovic, Thèse de Doctorat, Université Lyon-1, 1997 (unpublished).

[6] H.H. Andersen and J.F. Ziegler, in *The Stopping and Ranges of Ions in Matter*, edited by J.F. Ziegler (Pergamon Press, New York, 1977) Vol. 3.

[7] L.H. Toburen, Y. Nakai and R.A. Langley, Phys. Rev. **171**, 114 (1968).

[8] Y. Nakai, T. Shirai, T. Tabata and R. Ito, At. Data and Nucl. Data Tables **37**, 69 (1987).

[9] Y.K. Kim and K.T. Cheng, Phys. Rev. A **22**, 61 (1980).

[10] H. Ogawa, N. Sakamoto, I. Katayama, Y. Haruyama, M. Saito, K. Yoshida, M. Tosaki, Y. Susuki and K. Kimura, Phys. Rev. A **54**, 5027 (1996).

[11] P.M. Echenique, F. Flores and R.H. Ritchie, in *Solid State Physics, Advances in Research and Applications*, edited by H. Ehrenreich and D. Turnbull (Academic, New York, 1990), Vol. 43, p. 229.

[12] V.P. Shevelko, Z. Phys. A **287**, 19 (1978).

[13] M. Rødbro, E. Horsdal Pedersen, C.L. Cocke and J.R. Macdonald, Phys. Rev. A **19**,1936 (1979).

[14] K. Kroneberger, A. Clouvas, G. Schlüssler, P. Koschar, J. Kemmler, H. Rothard, C. Biedermann, O. Heil, M. Burkhard and K.O. Groeneveld, Nucl. Instrum. Methods Phys. Res. B **29**, 621 (1988).

[15] K. Kanaya and S. Ono, J. Phys. D: Appl. Phys. **9**, 161 (1976).

[16] S. Lencinas, J. Burgdörfer, J. Kemmler, O. Heil, K. Kroneberger, N. Keller, H. Rothard and K.O. Groeneveld, Phys. Rev. A **41**, 1435 (1990).

FIGURE CAPTIONS

Fig. 1: Experimental set-up.

Fig. 2: Projectile energy dependence of the backward electron yields measured with the thin and the thick carbon target, respectively. Measurements with incident protons were performed in coincidence with emergent protons and measurements with incident neutrals in coincidence with emergent protons and neutrals, respectively. The solid line is the fit of $\gamma_B(H^+,H^+)$ by the product $\Lambda_B S_e(H^+)$. The dotted lines are just to guide the eye.

Fig. 3: Same as Fig. 2, but for forward electron yields.

Fig. 4: Calculated energy dependence of the reconstituted H^0 fraction Φ_{0r}, of the transmitted H^0 fraction Φ_{0t}, and of their sum Φ_0, the neutral fraction at emergence from the thin target (tilted to 45°) bombarded by H^0 projectiles.

Fig. 5: Comparison between experimental data (full circles) and calculated values (open diamonds) of $\gamma_B(H^0,H^0)$ deduced from the weighted contributions of transmitted atoms (solid curve) and of reconstituted atoms (open triangles, see text). The dotted lines are just to guide the eye.

Fig. 6: Statistics of forward electron emission from the thin target under impact of 2.2 MeV projectiles, H^+ and H^0 (bars). Resulting distributions $W'_n(e_{proj})$ and $W_n(e_{proj})$ (see text).

Fig. 7: For H^0 projectile incident on the thin target, energy dependence of $\gamma_F(e_{proj})$, the mean number of forward emitted electrons per transmitted projectile electron (open circles), and of T_e, the probability of transmission of a projectile electron (full triangles). The dotted lines are just to guide the eye.

Fig. 1

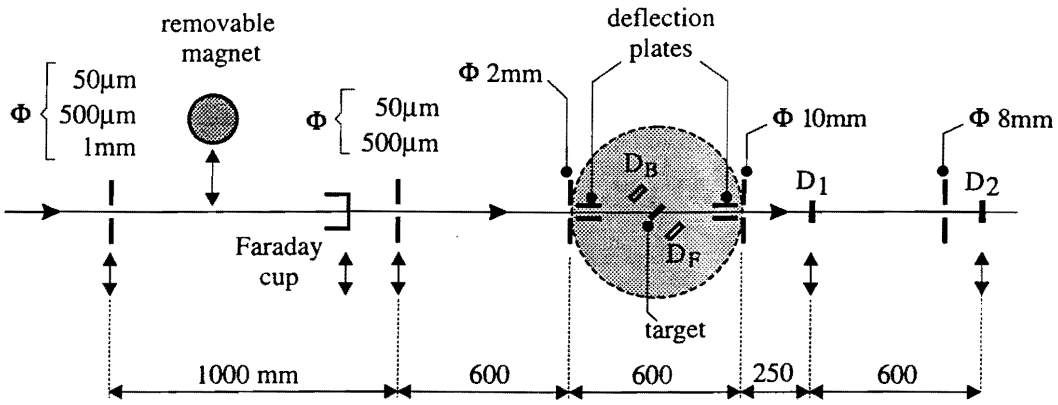

Z. Vidović - PRA -

Fig. 2

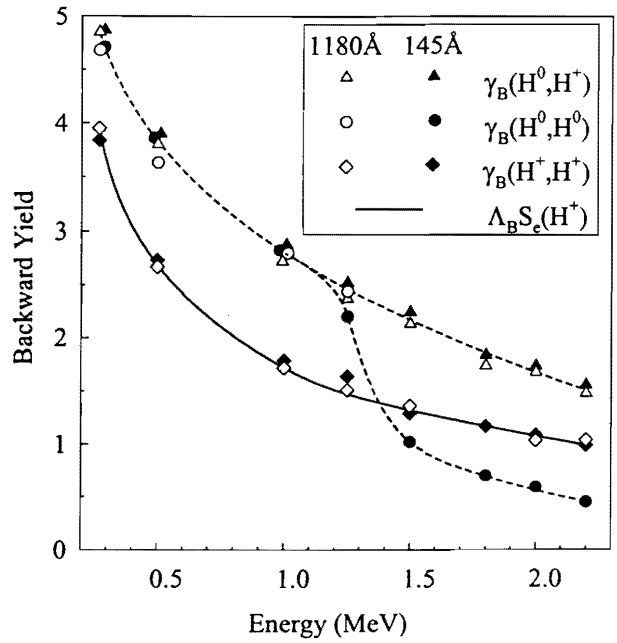

Z. Vidović - PRA -

Fig. 3

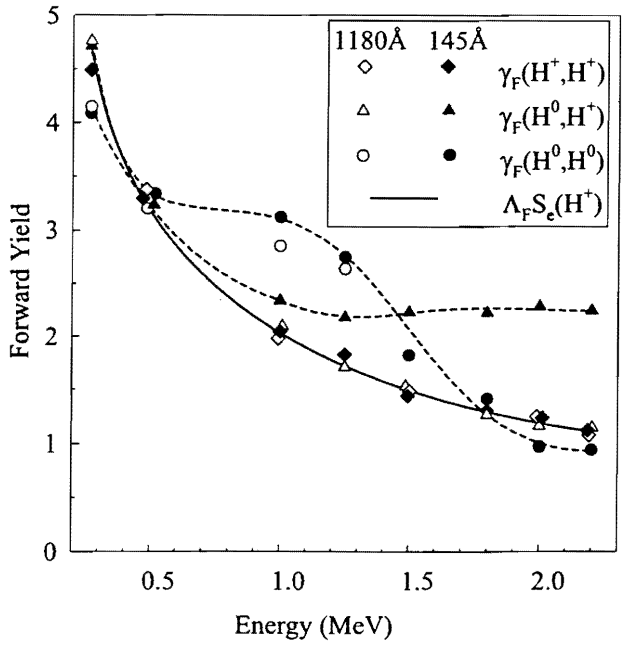

Z. Vidović - PRA -

Fig. 4

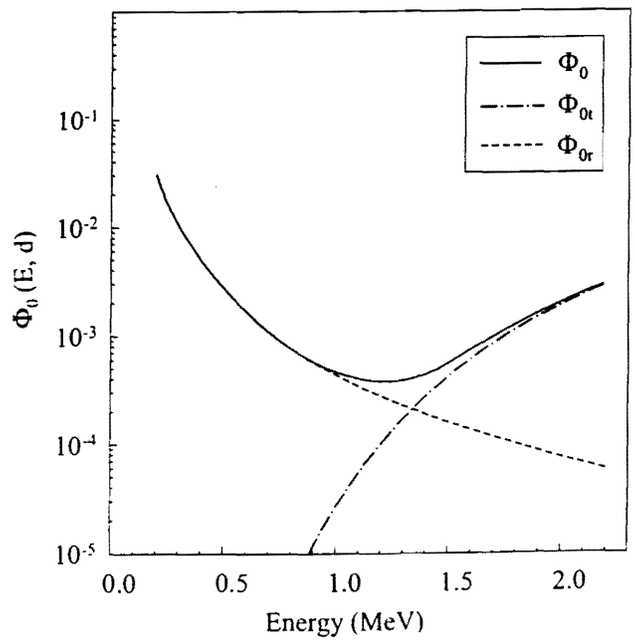

Z. Vidović - PRA -

Fig. 5

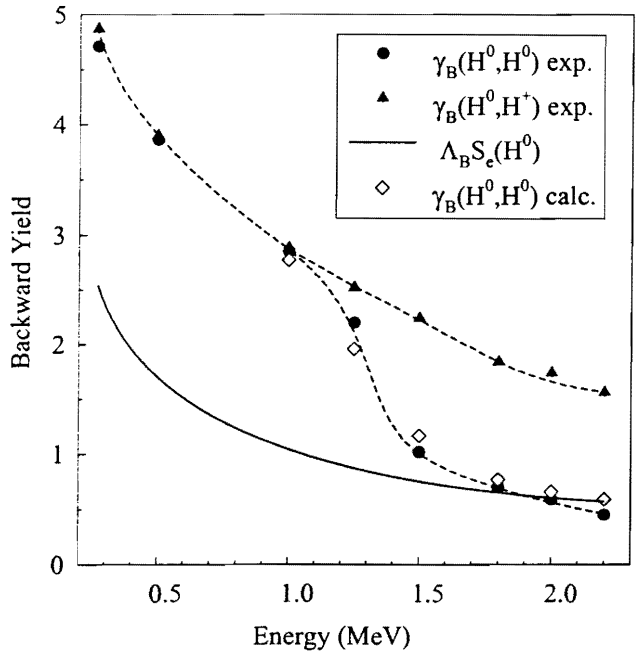

Z. Vidović - PRA -

Fig.6

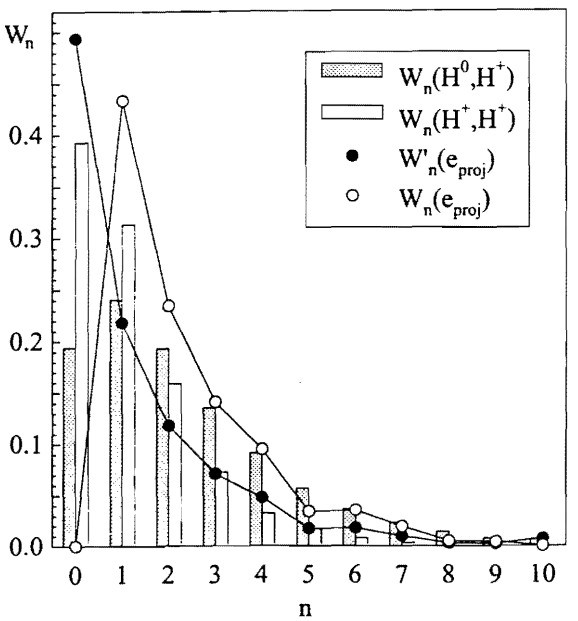

Z. Vidović - PRA -

Fig. 7

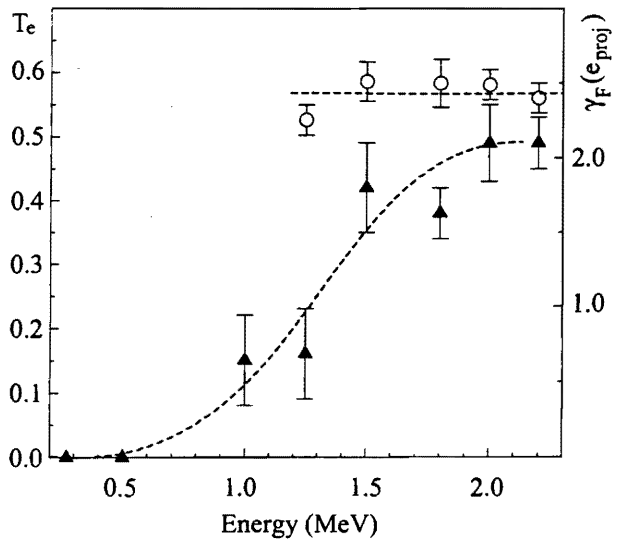

Z. Vidović - PRA -